International Conference on Space Optics—ICSO 2024
Antibes Juan-les-Pins, France
21-25 October 2024

Edited by Philippe Kubik, Frédéric Bernard, Kyriaki Minoglou and Nikos Karafolas

Tip-tilt Pre-Compensation Improvement by Adding a Gaussian Apodization Filter in the Rx Tracking Path

International Conference on Space Optics — ICSO 2024, edited by Frédéric Bernard, Nikos Karafolas, Philippe Kubik, Kyriaki Minoglou, Proc. of SPIE Vol. 13699, 136996E · © 2025 ESA and CNES · 0277-786X · doi: 10.1117/12.3075361

Tip-tilt Pre-Compensation Improvement by Adding a Gaussian Apodization Filter in the Rx Tracking Path

Rudolf Saathof*

Delft University of Technology, Department of Space Engineering,
Kluyverweg 1, the Netherlands

ABSTRACT

Tip-tilt pre-compensation adds a significant performance improvement for uplink optical communications channels, such as optical feeder-links. Besides the large contribution of tip-tilt to the wavefront disturbances, tip-tilt aberrations are less sensitive for the point ahead angle than higher order aberrations. Nevertheless, reciprocity between downlink and uplink is not perfect, resulting in residual pointing errors. One effect is the difference in beam shape: the downlink can be considered as a plane wave, whereas the uplink typically is a Gaussian beam. To improve reciprocity between up and donwlink, I propose to use a Gaussian apodization filter inn the part of the downlink beam that is used for measuring tip-tilt. This idea is tested using a numerical wave propagation simulation. In this simulation the reduction of beam wander is 13% and 20% is observed in the direction of the point ahead angle, and its transversal direction respectively. Also, it reduced the scintillation index by 8%. This yielded an improvement of the optical link by 1.5 dB at a probability of 10^{-3}.

Keywords: Optical Feederlinks, Tip-tilt Precompensation

1. INTRODUCTION

Optical feederlinks are foreseen to feed data to telecommunications satellites.[1] Although optical links have major advantages, such as improved throughput and security, there are also some drawbacks, such as cloud cover, that can block the optical communications beam,[2] and atmospheric turbulence. Atmospheric turbulence causes optical power decrease and power fluctuations in the receiver plane. This is due to: 1) beam wander and pointing jitter and 2) destructive and constructive interference, causing a speckle pattern.[3]

Beam wander can be significantly reduced by means of tip-tilt pre-correction.[4,5] Fig. 1 shows that the optical beam travels over a pointing system, consisting of a coarse pointing assembly (CPA) and fast steering mirror (FSM). This pointing system is controlled using a tracking detector, which measures the spot location of the incoming beam and a FSM that applies the physical correction. In this configuration, by correcting the received beam, also the transmit beam is pre-corrected. Pre-correction is improving the beam wander, but perfect correction cannot be obtained, because the up and downlink are not perfectly reciprocal. Sources of non-reciprocity are: 1) the point ahead angle (PAA); 2) the time delay of the control system and time of flight; and 3) the shape difference of the up-link and downlink beam. The lack of reciprocity due to the PAA is typically not compensated, but ideas exist to utilize laser guide stars.[6] Lack of reciprocity due to the time delay can be limited by a high control bandwidth. However, compensating the lack of reciprocity between the shape of beam has not been addressed yet.

In this paper, I propose a simple method to improve the uplink performance in Sec.2. The validity of this method and the performance increase is determined by means of a wave optics simulation in presented in Sec.3. The beneficial effects are presented in Sec.4, and conclusions on system level are drawn in Sec.5.

*E-mail: R.Saathof@TUDelft.NL

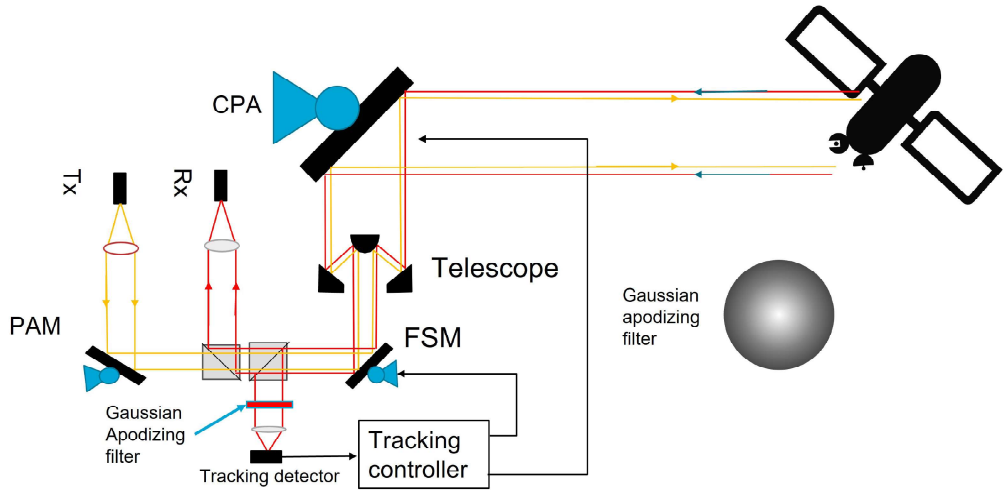

Figure 1. Typical system view of an optical communications terminal. As an addition, the Rx beam to the tracking detector has a Gaussian apodizing filter. The cross-section of the filter is in right part of the figure.

2. SYSTEM VIEW

The modified laser satcom system is depicted in Fig. 1. The received optical beam is typically a plane wave, since the satellite is sufficiently far away from the ground station. After passing through the telescope, and the pointing system, part of the beam irradiance is split off and redirected to the tracking detector. The uplink beam is typically a beam resembling a Gaussian shape, with some alterations, such as clipping, and is also indicated as Tx beam. Such a system typically has a point ahead mirror (PAM) to compensate for the point ahead angle (PAA).

Compensating the aberrations in the uplink beam to improve the quality and efficiency of communications, can be done by assuming reciprocity of the uplink beam compared to the downlink beam. Reflecting this to the shape of the beam, it means that either the uplink beam must be made similar to the downlink beam, or vice versa. As the profile of a laser beam is essential Gaussian, it is challenging to make it similar to the downlink, i.e. make it a flat-top beam, without inducing a lot of losses in the laser power. Hence, I propose to modify the downlink beam, but only the part that is measured for compensation, so the power for the data link So in the part of the beam, that is split off to the tracking sensor an apodizing filter is inserted, which is ideally conjugated to the pupil plane. The transmittance profile of this apodizing filter is matched to the Gaussian beam of the transmit beam. This creates a weighing to the received beam, so the center of gravity is matched better with the turbulence the optical beam travels through.

3. SIMULATION

3.1 Wave Optics Simulation

A wave optics numerical propagation simulation is defined in Matlab, using the split-step approach with the angular spectrum method.[7] The turbulence strength is defined by the Hufnagel Valley model, with $C_n^2(0) = 5 \cdot 10^{-14}$ m$^{-2/3}$ and $V_{RMS} = 42$ m/s. This results in a Fried parameter of 10 cm, an isoplanatic angle of 10 microradians at an elevation angle of 60 degrees and a wavelength of 1550 nm.

Discretization over the boresight is done by assuming random phase screens at 8 altitudes h using:[8]

$$h = \left[\begin{array}{cccccccc} 0 & 100 & 600 & 1250 & 2500 & 5800 & 10 \cdot 10^3 & 20 \cdot 10^3 & 40 \cdot 10^3 \end{array}\right] \text{m}. \quad (1)$$

The phase screens have an inner scale l_0 of 5 mm and an outer scale of 1000 m. The field has a diameter of 3 meters and a pixel size of 256×256. Nine sub-harmonic layers have been used, to have a representative amount of angle of arrival fluctuations. To avoid frequency leakage, a windowing function has been used, that has a flat top in the dominant part of the phase screen. The edge consists of half a period of a cosine function, with a

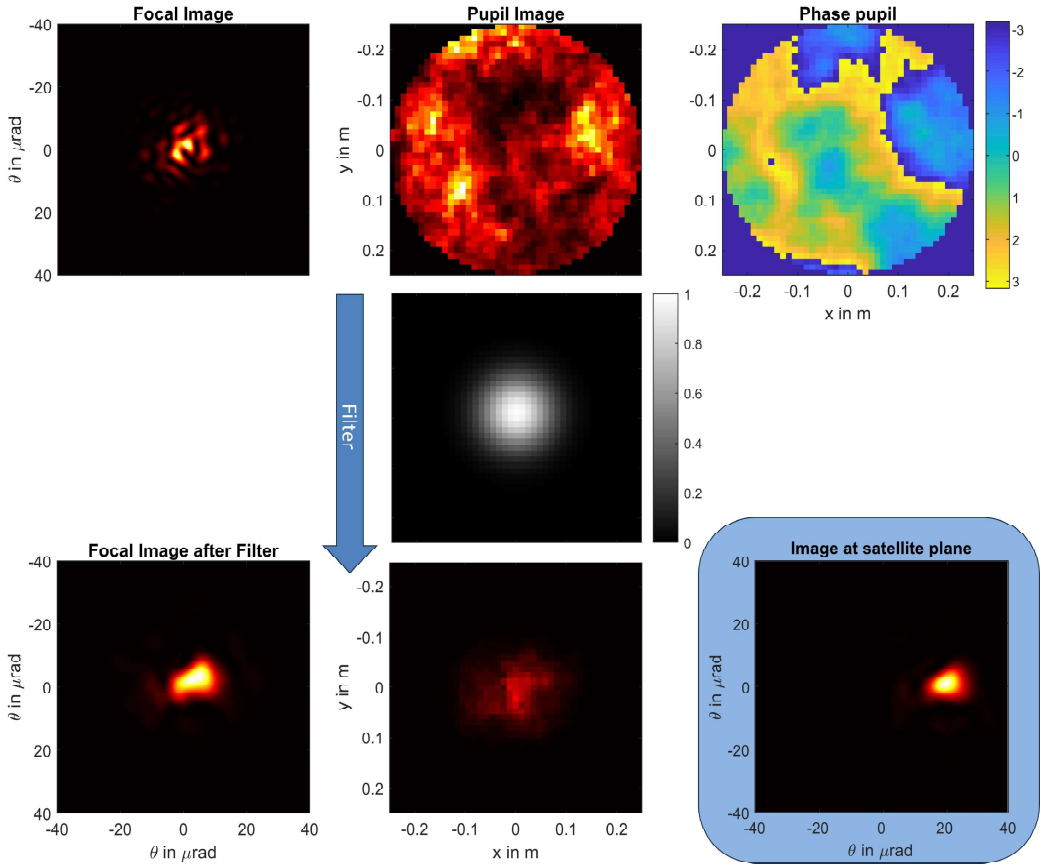

Figure 2. One sample of a wave propagation result and the simulation approach. The top row shows the focal plane image, pupil plane image and phase field in the pupil of telescope. The figure in the center shows the filter function that is applied on the electrical field. The middle picture in the bottom row shows the pupil image after filtering, and the left lower corner Irradiance values have an arbitrary scales, since they are dependent on the laser power of the source, which is irrelevant for this paper.

nominal width of 32 pixels. As the field is significantly larger than the dimensions of the optical beam, tip-tilt aberrations are sufficiently represented in the phase screens. The amplitude of the phase screens have been scaled using the partial Fried parameter:

$$r_{0,i} = \left[0.423k^2 \sec\zeta \int_{h_i}^{h_{i+1}} C_n^2(z)dz\right]^{-3/5} \tag{2}$$

with k the wave number, ζ the zenith angle of 30 degrees, C_n^2 the refractive index structure parameter and z the propagation distance over the link.

The downlink is assumed to be a plane wave, which is a good approximation, since the satellite is sufficiently far away from the atmosphere. Hence, the scaling can be validated using Noll:[9]

$$\sigma_\theta^2 = (D/r_0)^{5/3} \tag{3}$$

In which σ_θ^2 is the variance of the wavefront errors, D the diameter of the receiving aperture, and r_0 the Fried parameter over the entire link. The results fit within a percentile between the analytic equation and the numeric propagation. Another model verification is done by comparing the scintillation index of the downlink in the pupil plane with the analytic form:

$$\sigma_I^2 = 2.25k^{7/6} \sec^{11/6}(\zeta) \int C_n^2(z) z^{5/6} dz, \tag{4}$$

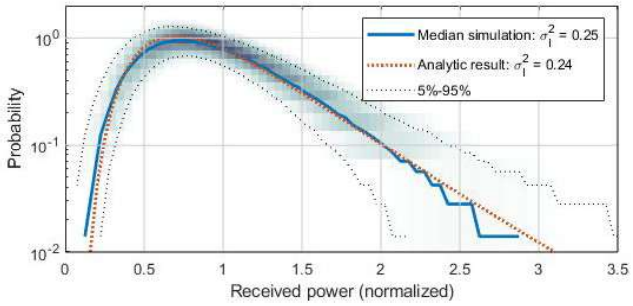

Figure 3. Verification result of the wave propagation simulation on the downlink by means of the scintillation index and the log-normal distribution.

and is compared to a log-normal distribution in Fig.3 In addition to the downlink, also the projection on the focal plane is obtained. This is one by Fraunhofer propagation. An example of the Pupil image, phase, and focal image is depicted in Fig. 2

The uplink beam has a Gaussian shape, with a $1/e^2$ waist radius of 10 cm, and no defocus. To simulated an uplink scenario to a Geostationary satellite, a point ahead angle of 18.6μrad is taken. From the point of the top of the atmosphere (40 km altitude) to the satellite the beam is propagated using Fraunhofer propagation. This assumes the satellite is in the far field, which is a valid assumption, as the Fraunhofer region is about 500 km, for beam diameter of 1 m. I.e. this simulation also is valid for propagation to a low earh orbit (LEO) satellite. Result of one propagation to the satellite is shown in Fig. 3

3.2 Tip-tilt compensation

The simulation of tip-tilt control is done by assuming no servo-delay error or sensor noise. So the only errors originate from the combination of the algorithm used to determine tip-tilt and the limited reciprocity between the uplink and downlink. The simulations labeled as open loop have no tip-tilt compensation. As a reference case, the simulations labeled as spot location use an aperture size of 2.1× the waist radius of the uplink beam (i.e. 10.2 cm). The spot location is determined using the center of gravity algorithm:

$$x_{COG} = \frac{\sum x_d I_d(x_d, y_d)}{\sum I_d(x_d, y_d)}, \tag{5}$$

resulting in $I_d(\theta_{x,d}, \theta_{y,d})$, with $\theta_{x,d}, \theta_{y,d}$ the coordinates in the detector plane. The so determined amount of tip-tilt is added to the phase of the Gaussian beam. This tip-tilt corrected Gaussian shape is used as input for the uplink of the reference case.

To test the idea posed in this paper, i.e. in Section 2, the pupil plane image of the downlink is first spatially filtered with the Gaussian profile, that is also used for the uplink. Next it is propagated to the image plane of the telescope by means of Fraunhofer propagation. To estimate the amount of tip-tilt, the center of gravity algorithm of Eq. 5 is used again. These simulations are labeled as Weighted spot location.

3.3 Other metrics used

When projected on the satellite plane, the spot position is estimated using the center of gravity algorithm is used (similar to Eq. 5.). Also, the irradiance at the average beam position is captured, to obtain the scintillation index, and the probability density function (PDF) of the irradiacne fluctuations in the satellite plane. To estimate the advantage of this method, the cumulative density function (CDF) is derived from the PDF. The advantage of the proposed method is determined by manually assessing the CDF, by the fraction of irradiance between the CDF of the weighted spot location and the spot location. As good practice, this is expressed in dB ($10\log_{10}(\cdot)$).

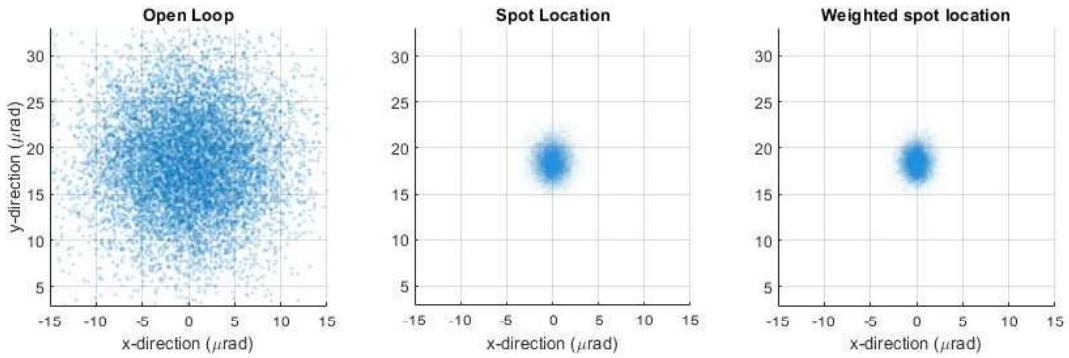

Figure 4. Scatter plots of the simulation results of the location of the uplink beam, as determined by the center of gravity algorithm for all three cases.

4. RESULTS

4.1 Beam wander reduction

Fig. 4 shows the scatter plots of the open loop, the spot location and the weighted spot location. Immediately visible is the reduction of beam wander from open loop to closed loop, by almost 1 order of magnitude. Nevertheless, there is beam wander left, which is caused by limited reciprocity of the downlink compared to the uplink. Also remarkable, is that the scatter plots of the corrected beam wander are elliptical. This is because along the line of no point ahead angle, the reciprocity is better compared to the direction of the point ahead angle. When carefully assessing the difference between spot location and weighted spot location a slight difference between the spot location, and weighted spot location can be observed, but is not super obvious. Hence, this is assessed in more detail using a histogram.

The in depth assessment of the improvement of beam wander is shown in Fig. 5. Also in these plots, it is immediately visible how much of an improvement tip-tilt pre-correction yields. In these plots, also the difference between the spot location and weighted spot location is visible, mainly in the height of the curve, which corresponds also to the narrowing of the curves. To emphasize this, also the numeric values are shown in the legend and presented in Table 1. It first shows that standard deviation of the weighted spot location is clearly lower than the spot location. The improvement in the non-PAA direction is 20% and in the PAA direction it is 12%. This is also reflected in the rotational symmetry of scatter plots. For the spot location simulation, the beam wander is in the PAA direction 22% more compared to the non-PAA direction, whereas this difference is 30% for the weighted spot location. This is due to the better reciprocity of the non-PAA direction. These results show there is moderate improvement of the beam wander by applying the Gaussian apodization filter in the pupil plane, before the tracking detector.

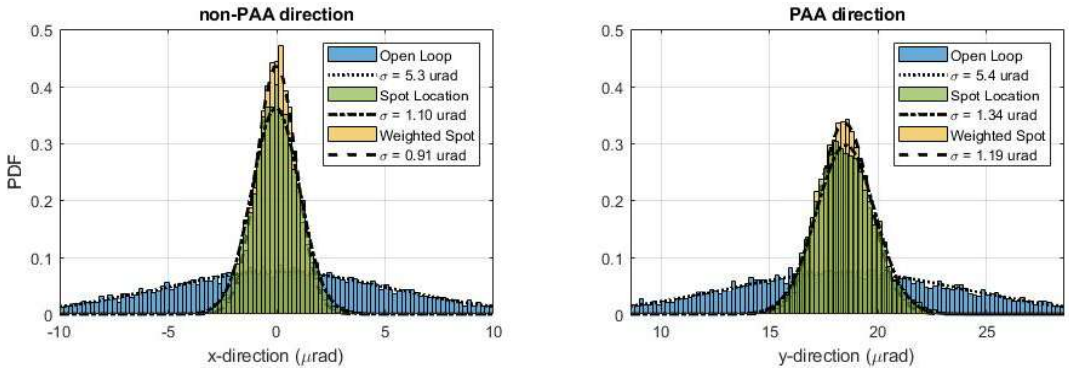

Figure 5. The probability densities of the beam wander, over the axis in the direction of the point ahead angle (PAA), and in the transversal direction.

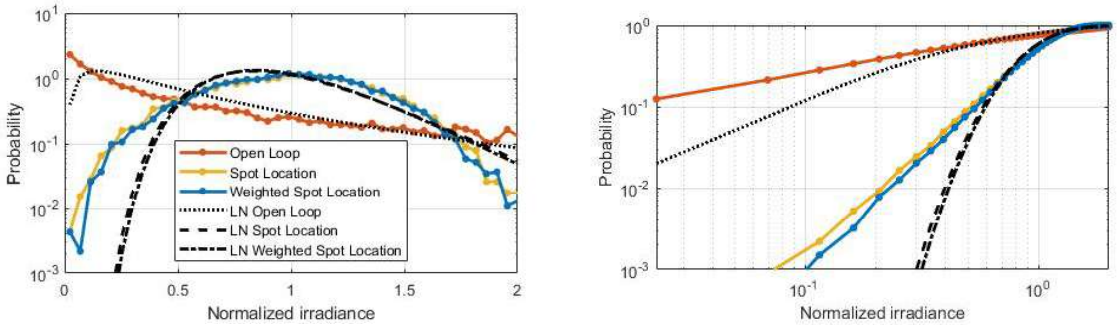

Figure 6. Left: probability density of the irradiance fluctuations, on a semi-logarithmic scale. Both the wave propagation result, and the log normal distribution based on the analytically determined scintillation index are shown. Right: the CDF on a double logarithmic scale.

4.2 Irradiance statistics

For the commmunications link, the irradiacne fluctuations are more relevant than the beam wander fluctuations. To start the comparison, the scintillaion indices are shown in Table 1, which shows that the strong irradiance fluctuations of the open loop, are reduced to weak fluctuations by using tip-tilt pre-compensation. Also, the reduction of scintillation index using the weighted spot location algorithm is 8% lower than the spot location algorithm. Hence, it already shows that the apodization filter yields in a moderate improvement of the irradiance statistics of the uplink.

This is further detailed out in the probability density analysis in Fig. 6. The first obvious observation again is the significant improvement from the open loop to the closed loop setting. From the statistics it is shown that in open loop the link is almost impossible to work with, from a communications perspective. Also the known observation, that a log-normal distribution cannot represent the statistics well, is clear from this plot. In particular, it underestimates the effect of scintillation for lower probabilities. The differences in the PDF between the two correction algorithms show that the weighted spot location is slightly favourable for low probability and normalized irradiance. This is further detailed out in the CDF, which shows that the curves are diverging for lower probabilities. As can be read from Table 1, the advantage is 1.5 dB for a fade probability of 10^{-3}. As the number of samples used in this simulation is not sufficiently large, it is not shown in this paper, but it can be speculated that for lower fade probabilities, the advantage can reach to several dBs. Hence, a moderate improvement of the link statics can be improved by a low cost and simple adaptation to the tip-tilt pre-correction system only.

Filter	Std x (μrad)	std y (μrad)	σ_I^2	$\tilde{I}$ at 10^{-3}
Open loop	5.3	5.4	1.33	n.a.
Spot location	1.10	1.34	0.12	0.10
Weighted spot location	0.91	1.19	0.11	0.07
Improvement	20%	13 %	8%	1.5 dB

Table 1. Numerical simulation results.

5. CONCLUSION

In this paper I propose to add a apodization filter in the Rx path that runs to the tracking detector to improve the irradiance statistics for the uplink beam. The effect of this is analysed by means of a wave propagation simulation. This is done by improving reciprocity, that reduces the beam wander by 12-20% for in the direction of the PAA angle transversal respectively. Also remarkable, but logical, is that the scatter plot of the beam positions shows an ellipsoid shape, because the reciprocity is assymmetric. Regarding the irradiance statistics, the improvement of the reciprocity reduces the scintillation index by 8%. This results in a 1.5 dB improvement at a fade probability of 10^{-3}. Hence, the simple and cost effective addition of the apodization filter in the pupil plane in the Rx of the tracking system, yields a moderate improvement of the optical link.

REFERENCES

[1] Saathof, R., den Breeje, R., Klop, W., Kuiper, S., Doelman, N., Pettazzi, F., Vosteen, A., Truyens, N., Crowcombe, W., Human, J., Ferrario, I., Calvo, R. M., Poliak, J., Barrios, R., Giggenbach, D., Fuchs, C., and Scalise, S., "Optical technologies for terabit/s-throughput feeder link," in [*2017 IEEE International Conference on Space Optical Systems and Applications (ICSOS)*], 123–129 (2017).

[2] Poulenard, S., Crosnier, M., and Rissons, A., "Ground segment design for broadband geostationary satellite with optical feeder link," *J. Opt. Commun. Netw* **7**(4), 325–336 (2015).

[3] Andrews, L. and Phillips, R., [*Laser beam propagation through random media*], SPIE press (2005).

[4] Fried, D. L., "Anisoplanatism in adaptive optics," *Journal of the Optical Society of America* **72**(1), 52 (1982).

[5] Alaluf, D., Armengol, J. M. P., Sodnik, Z., and Technology, E. S., "How effective is tip-tilt pre-compensation for optical uplinks based on the received downlink optical signal ?," in [*ICSO*], (2019).

[6] Mata-Calvo, R., Bonaccini Calia, D., Barrios, R., Centrone, M., Giggenbach, D., Lombardi, G., Becker, P., and Zayer, I., "Laser guide stars for optical free-space communications," *Proc. of SPIE Vol* **10096**, 100960R (2017).

[7] Schmidt, J. D., [*Numerical simulation of optical wave propagation with examples in MATLAB*], SPIE (2010).

[8] Charnotskii, M., "Comparison of four techniques for turbulent phase screens simulation," *JOSA A, Vol. 37, Issue 5, pp. 738-747* **37**, 738–747 (may 2020).

[9] Noll, R. J., "Zernike polynomials and atmospheric turbulence," *Journal of the Optical Society of America* **66**, 207 (mar 1976).